



Mesoporous silicon photonic structures with thousands of periods

Sergey E. Svyakhovskiy, Anton I. Maydykovsky, and Tatiana V. Murzina

Citation: *J. Appl. Phys.* **112**, 013106 (2012); doi: 10.1063/1.4732087

View online: <http://dx.doi.org/10.1063/1.4732087>

View Table of Contents: <http://jap.aip.org/resource/1/JAPIAU/v112/i1>

Published by the [American Institute of Physics](#).

Related Articles

Extraordinary blueshift of a photonic crystal nanocavity by reducing its mode volume with an opaque microtip
Appl. Phys. Lett. **101**, 051102 (2012)

Giant field localization in 2-D photonic crystal cavities with defect resonances: Bringing nonlinear optics to the W/cm² level
AIP Advances **2**, 032112 (2012)

Guided-wave-coupled nitrogen vacancies in nanodiamond-doped photonic-crystal fibers
Appl. Phys. Lett. **101**, 031106 (2012)

Photonic band structures of one-dimensional photonic crystals doped with plasma
Phys. Plasmas **19**, 072111 (2012)

Enhancing the locality of optical interrogation with photonic-crystal fibers
Appl. Phys. Lett. **101**, 021114 (2012)

Additional information on J. Appl. Phys.

Journal Homepage: <http://jap.aip.org/>

Journal Information: http://jap.aip.org/about/about_the_journal

Top downloads: http://jap.aip.org/features/most_downloaded

Information for Authors: <http://jap.aip.org/authors>

ADVERTISEMENT

IBD Optical Film Quality at PVD Rates

Advanced Optical Thin Films

Wide Range of Applications

Superior Throughput and Repeatability

SPECTOR-HT ION BEAM DEPOSITION SYSTEMS

Veeco

Innovation. Performance. Brilliant.

www.veeco.com/spectorht

Mesoporous silicon photonic structures with thousands of periods

Sergey E. Svyakhovskiy,^{a)} Anton I. Maydykovsky, and Tatiana V. Murzina
Department of Physics, M.V. Lomonosov Moscow State University, 119991 Moscow, Russia

(Received 2 May 2012; accepted 24 May 2012; published online 5 July 2012)

In this work, we present the results on the fabrication and characterization of the structural and optical properties of thick mesoporous silicon-based 1D photonic crystals (PC) containing up to 2500 periods (400 μm thick) made by electrochemical etching in the hydrofluoric acid solution. The composition of multilayered structures with good spatial periodicity up to thousands of layers and with good reproducibility of porosity of alternate layers is demonstrated that is proven by SEM measurements. Comparative studies of the reflectivity spectra from the front and back sides of a thick free-standing PC also testify a good periodicity of the multilayer structure which manifests itself by the appearance of the photonic band gaps. We demonstrate that the main mechanism that restricts the fabrication of thick porous silicon-based photonic crystals is the local decreasing of the HF concentration in pores. © 2012 American Institute of Physics. [<http://dx.doi.org/10.1063/1.4732087>]

I. INTRODUCTION

Wave propagation in periodic structures has been intensively studied for a long time.¹ A renaissance in the interest in this area traces back to the end of the last century after the appearance of the paper by Ref. 2, where the concept of photonic crystals (PC) was announced. Since that time, a number of new effects were observed in PC such as an enhancement of nonlinear optical effects, Borrmann effect, slow light, and enhanced emission.^{3,4}

Among various methods for the fabrication of photonic crystals, a special place belongs to porous silicon (PS) based technique.⁵ Numerous studies⁶ have demonstrated that in case of crystalline silicon with the surface orientation (001), the electrochemical etching results in the formation of pores growing in the direction perpendicular to the surface. The surface densities of pores that are being randomly formed on the silicon surface as well as the porosity factor, i.e., the volume fraction of air in the PS structure, are controlled by the etching parameters.⁷ In particular, a multilayer structure can be composed by the temporal modulation of the etching current as the layers with different porosities, i.e., with different refractive indexes, are formed. The PS layers are oriented parallel to the surface plane thus forming a periodic structure in the direction that is normal to the surface or one-dimensional (1D) photonic crystal. The thickness of the layer is determined by the etching time and surface density of current.

Recently, a number of theoretical works appeared where novel effects like spatial and temporal splitting of ultrashort laser pulses⁸ and the optical echo⁹ were predicted. At the same time, practical implementation of these effects has been lacking mostly due to a problem of fabrication of the PC structures containing several hundreds of layers. The most common fabrication techniques can hardly be applied for the realisation of this task, so it was the main motivation of our study: acoustic standing waves¹ cannot provide high

refraction index contrast; holography and photopolymerization^{10,11} cannot provide high refraction index contrast and high aspect ratio in one-dimensional case; spin coating^{12,13} and spray coating¹⁴ cannot provide stable structures of high number (100+) of periods.

In this paper, we present the results of the consecutive study of the electrochemical etching procedure of porous silicon PCs and demonstrate that under special efforts these can be used for the fabrication of rather thick (up to several thousands of spatial periods) 1D photonic crystals. The paper is organized as follows. Section II contains the description of the main experimental details of the electrochemical etching procedure; in Sec. III, conditions of the stability of the etching process are studied and the influence of the hydrofluoric acid concentration inside the pores on the parameters of thick PC is described. In Sec. IV, structural and optical properties of porous silicon structures are observed. Section V deals with the unique properties of annealed porous silicon based PC, followed by conclusions.

II. EXPERIMENTAL PROCEDURES

Porous silicon samples were fabricated by the electrochemical etching of a p-type Si(001) wafers with the resistivity of $0.002 \div 0.005 \Omega\text{-cm}$ in the electrolyte HF:H₂O:ethanol in proportion of 2:4:3 (HF concentration of 21% (w/w)) unless otherwise stated. Silicon wafers were placed in a cylindrical two-electrode electrochemical cell, where the Si plate was used as the bottom electrode while a Pt wire as the top one. The cell volume was approximately 20 cm³ and the area of the silicon anode exposed to the etchant was about 1.76 cm². The electric current density during the etching process was modulated by a computer-controlled galvanostat P-5848.

The electrochemical etching results in the formation of pores with the average diameter of about $10 \div 60 \text{ nm}$ growing in the direction perpendicular to the Si (001) surface. In our experiments, photonic crystals were composed of a set of two layers of high refractive index n_1 and the thickness d_1 (low porosity layer) and of low refractive index n_2 and the

^{a)}Electronic mail: sse@shg.ru.

thickness d_2 (high porosity layer). The etching current densities used for the composition of these layers were $j_1 = 10 \text{ mA/cm}^2$ and $j_2 = 100 \text{ mA/cm}^2$, respectively. Multilayer photonic crystals were composed by a consecutive repetition of the necessary number of etching cycles as the time and current density were fixed. The largest number of layers we composed was 5000. The average thickness of the sample was about $400 \mu\text{m}$ and was restricted only by the thickness of the silicon plate. The schematic view of the etching cell is shown in Fig. 1. In order to make a free-standing PC, it was released from the Si(001) substrate by a pulse of etching current of about 1 A/cm^2 .

The etching procedure was automatized using a LabVIEW (National instruments) computer program that was applied to control the etching process.

It is known from the literature¹⁵ that one of the main difficulties in the composition of thick PC using the electrochemical etching procedure is the decrease of the etching rate in of the deep PS layers. In order to avoid this, we have introduced a mixing system within the cell intended to improve the electrolyte circulation within the pores. This system consists of mixing fan placed above platinum electrode and an orbital shaker on which cell is mounted (Fig. 1). The rotation of the orbital shaker enables the flow of the etchant and provides an interfusion of the solution. The rotation rate was selected to obtain the proper quality of the sample but should not exceed the threshold while the flow remains laminar. Below, we compare the structural and optical properties of the PC samples made using this system and without it.

Optical properties of the samples were characterized by measuring their transmission or reflectivity spectra using a set-up based on the spectrometer ASP-100 M. The optical excitation of the structure was performed using a halogen lamp which provided the illumination of the examined structure in the wavelength range from 400 nm up to 1000 nm . The calibration of the reflectivity spectra of the sample over the excitation spectrum of the lamp was carried out in all the measurements.

III. CALIBRATION OF THE ETCHING PROCEDURE

In order to develop a reliable electrochemical technique for the fabrication of a photonic structure with desired parameters, we have performed a set of calibration measurements for uniform porous silicon films. Namely, the dependence of the etching rate on HF concentration was

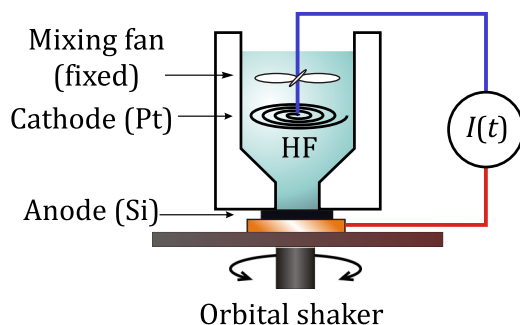


FIG. 1. The schematic view of the electrochemical cell.

measured, the dependencies of homogeneous PS film thicknesses on the etching time and the value of the etching current as well as the PS porosity on the etching current and time were revealed. The results of such a calibration were used later for a proper choice of the etching conditions for a composition of PS-based photonic crystals.

A. Estimation of porous silicon film thickness

First of all, it was necessary to develop a reliable probe of the thickness of the PS film. We have implied two methods: (1) a direct measurement based on the observation of the sample cleavage in an optical microscope and (2) the analysis of the spectral interference pattern of the reflected light. In our studies, we used both of them, while in spite of a relative simplicity of the second one we will discuss it in more detail. The point is that in order to estimate correctly the thickness of a PS layer from the reflectivity spectra one needs to know the dispersion of the refractive index of the porous silicon layer, which in turn depends on the porosity. In an effective medium approximation, the refractive index of a porous silicon layer of a constant porosity f , i.e., the bulk concentration of air, can be calculated from Bruggeman formula¹⁶ for the effective dielectric constant of a silicon-air porous media

$$(1-f) \frac{\epsilon_{Si} - \epsilon_{eff}}{2\epsilon_{eff} + \epsilon_{Si}} + f \frac{\epsilon_{air} - \epsilon_{eff}}{2\epsilon_{eff} + \epsilon_{air}} = 0, \quad (1)$$

where $\epsilon_{Si} = n_{Si}^2$ and $\epsilon_{air} = n_{air}^2$ are the dielectric function of silicon and air, respectively.

The reflectivity spectrum of a homogeneous film depends on its thickness d and the effective refractive index $n_{eff} \equiv n(\lambda)$ and is determined by a well-known expression:

$$R(\lambda) = 1 + \cos\left(\frac{4\pi nd \cos \theta}{\lambda}\right), \quad (2)$$

where θ is the angle of incidence of the light beam. For the sake of simplicity, we will assume below $\theta = 0$ and $nd \gg \lambda$, where λ is the wavelength of light. In the first approximation, $n(\lambda) = const$ and the expression for the optical thickness of the PS film takes the form

$$n(\lambda_k)d = \frac{1}{2} \left(\frac{1}{\lambda_i} - \frac{1}{\lambda_{i+1}} \right)^{-1}, \quad (3)$$

where λ_i and λ_{i+1} are the wavelengths that correspond to the neighbour interference maxima. For the case of $n(\lambda) \neq const$

$$d = \frac{1}{2} \left(\frac{n(\lambda_i)}{\lambda_i} - \frac{n(\lambda_{i+1})}{\lambda_{i+1}} \right)^{-1}. \quad (4)$$

It stems from Eq. (4) that PS layer thickness d can be estimated from the reflectivity measurements if the dispersion $n(\lambda)$ is known. In case of porous silicon, the function $n(\lambda)$ is determined by the dispersion of silicon $n_{Si}(\lambda)$ and the porosity f . As the function $n_{Si}(\lambda)$ is well known,¹⁷ the approximation 4 for different interference maxima can be applied for the estimation of the f value. Thus, both the thickness of a

homogeneous porous silicon-based films and their porosities were determined from the reflectivity spectra.

We have applied this method for the estimation of d and f and have proven its validity by comparing the values of these quantities with those obtained from the direct structural measurements. It should be noted that the described procedure is quite convenient as it allows to determine these parameters without performing SEM or AFM studies for each particular sample.

B. Depth dependence of the etching rate on the etching depth and current density

The dependencies of the optical (nd) and physical (d) thickness of homogeneous porous silicon films on the etching time τ are shown in Fig. 2. The values nd and d were estimated from both the optical reflectivity measurements and the optical microscopy. When fabricating the samples of homogeneous PS films for these measurements we used the electrochemical cell with the mixing system. One can see that the obtained dependencies are linear within the experimental accuracy. This correlates with the results obtained previously by other authors and allows to introduce the etching rate r that is determined as the ratio $r = d/\tau$.

Moreover, an important result here is that the refractive index of a porous silicon film remains nearly constant up to the thickness of $d = 50 \mu\text{m}$, which means that the porosity of the PS layer remains constant at such film thickness. This result supports the idea of a sufficient improvement of the proposed etching technique.

As the next step, the dependence of the etching rate r on the current density was measured; the obtained dependence is shown in Figure 3. It can be seen that r is a linear function of j in the whole accessible range of the current densities up to 200 mA/cm^2 .

It is worth noting that the linear character of $d(\tau)$ dependence is very important for the fabrication of PS-based photonic crystals. It allows to provide the required thickness of a PS layer with fixed porosity by controlling the etching

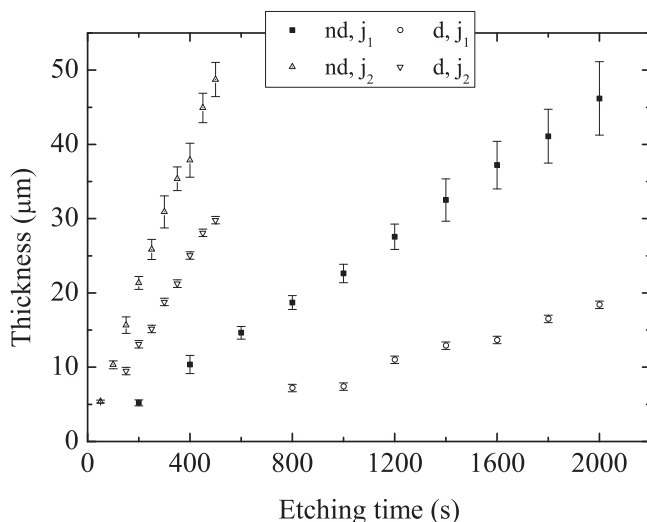


FIG. 2. The dependence of the optical (nd) and physical (d) thickness of porous silicon films on the etching time for current densities of $j_1 = 10 \text{ mA/cm}^2$ and $j_2 = 100 \text{ mA/cm}^2$, HF concentration of 21 wt. %.

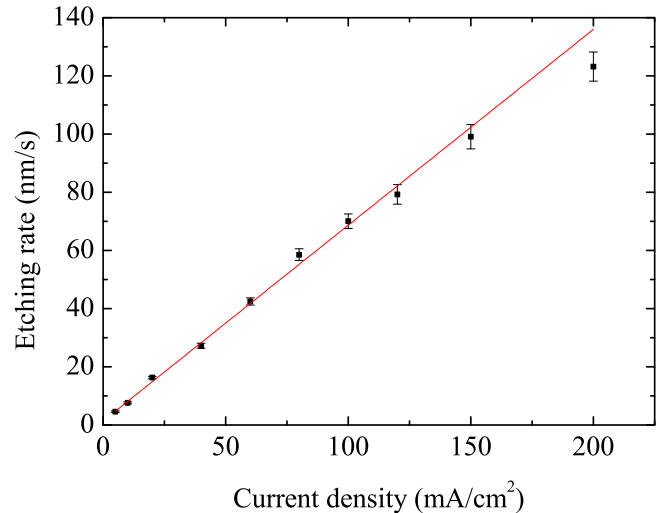


FIG. 3. The dependence of the PS etching rate on the current density, HF concentration of 21 wt. %.

time if all the other etching parameters are fixed. This is exploited in our computer-controlled experimental procedure of the fabrication of photonic crystals. Prior to making a photonic crystal, we performed the necessary calibration measurements for each type of Si(001) wafers and the electrolyte in order to estimate the etching rates r_1 and r_2 that correspond to the two chosen values of the etching current j_1 and j_2 (i.e., n_1 and n_2). After that, the parameters $j_1, j_2, r_1,$ and r_2 are introduced in the computer program which controls the electrochemical etching procedure to achieve the ratio $n_1 d_1 = n_2 d_2 = \lambda/4$, where λ is the central wavelength of the photonic band gap (PBG).

C. The role of HF concentration

It was mentioned above that the main problem in the fabrication of thick PS-based structures is the decrease of the etching rate r with the increase of the thickness of the porous layer d . We have also observed this effect when making porous silicon films or PC without mixing the solution during the electrochemical etching. As all the other parameters of the etching are controlled during the fabrication of the sample, it is evident that the decrease of r is caused by the reduction of the HF concentration participating in the process.

The reduction of the HF concentration can take place (1) in the bulk of the solution due to a fast acid consumption during the reaction and (2) a *local* reduction of the HF acid concentration at the bottom of pores due to a low convection rate of the electrolyte within the pores.

Simple estimations prove that the relative change of HF bulk concentration during the fabrication of thick PS-PC is less than 4%. It is known that in accordance with the reaction stoichiometry,⁶ 4 moles of HF are required for the anodization of one mole of silicon. During the etching of a PS layer of $400 \mu\text{m}$ thick and of the porosity of ~ 0.5 about 0.002 moles of Si is anodized, which requires about 0.008 moles of HF. Taking into account the volume of the electrochemical cell (20 cm^3) and the concentration of hydrofluoric acid in the solution (about 21% (w/w) volume fraction), it gives about 0.2 moles of HF. Thus, the possible decrease of the

bulk concentration should be rather low, about 0.04 (down to approximately 20%). This means that the main effect in the decrease of the etching rate in case of thick PS-based samples is the local reduction of the acid concentration within the pores.

In order to keep the HF concentration in pores the same as in the cell volume a mixing system was introduced in the electrochemical cell, as has been mentioned in Sec. II. The idea was that such a procedure provides a certain constant flow of the electrolyte in pores, thus only a rather small average bulk reduction of the HF concentration in the solution would affect the etching process.

To prove this assumption, we checked by SEM measurements that under the constant parameters of the electrochemical etching and when mixing the electrolyte during the fabrication the porosity of a PS film remains constant over the whole film thickness. We have also measured the dependence of the PS etching rate on the HF concentration. The corresponding dependence is shown in Figure 4. It can be seen that $d(\tau)$ dependence is linear within the experimental accuracy within the variation range of the experimental parameters. This property is also used for the controllable growth of porous silicon structures with desired parameters.

The most convenient way to check the mechanical mixing of this was to make a thick PS-based photonic crystal with constant values τ_1, j_1 and τ_2, j_2 . Modification of the microstructure of such samples with the thickness and the corresponding changes of their optical properties should reveal the HF concentration decrease. Such an experiment is described in the next section.

IV. CHARACTERIZATION OF THE MICROSTRUCTURE AND OF THE OPTICAL PROPERTIES OF THICK PS-BASED PHOTONIC CRYSTALS

The main approach for the fabrication of PS-based photonic crystals is a periodic in time variation of the current density and the etching time. We used the estimated values r and f and optimised the optical thickness of the layers in order to meet the requirement $n_1 d_1 = n_2 d_2 = \lambda/4$, where λ is

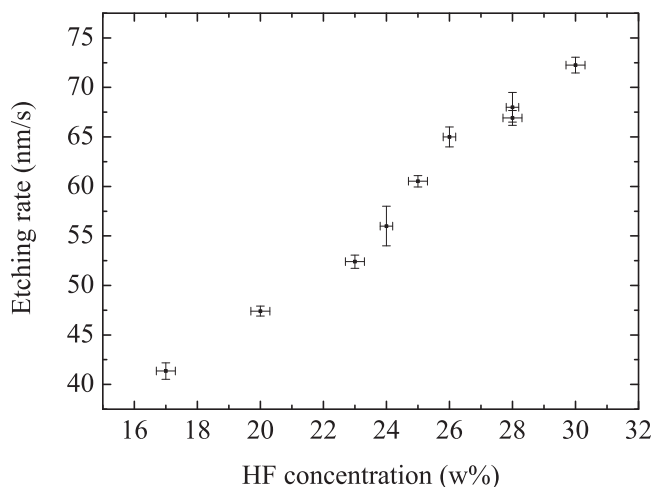


FIG. 4. The dependence of the etching rate of porous silicon films on the HF concentration for $j = 100 \text{ mA/cm}^2$; the mechanical mixing of the electrolyte during the electrochemical etching was realised.

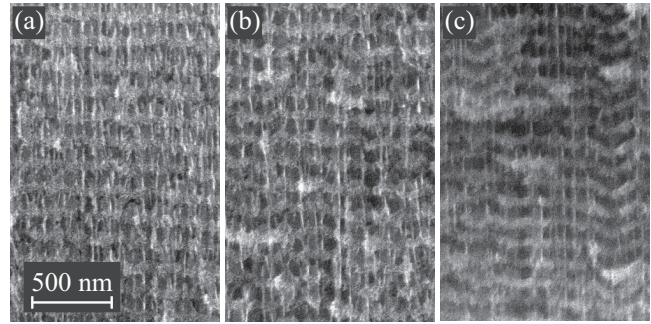


FIG. 5. SEM image of the porous silicon photonic crystal (PC-I) cleavage (side view, layers are horizontal, etching direction is from top to bottom) (a): for the layers with the numbers 1 ÷ 25 (front side), (b): layers in the middle of the sample, and (c): layers placed close to the back side of the PC (numbers 988 ÷ 1000).

the central wavelength of the desired photonic band gap. We made two sets of free-standing photonic crystals each of them composed of several thousands of layers. Estimated periods $D = d_1 + d_2$ of the structures were $D_{I,II} = 0.16 \mu\text{m}$. The first and the second sets of samples (referred below as PC-I and PC-II, respectively) were made without and with the mixing of the electrolyte, respectively.

Figure 5 shows the SEM images of the cleavage of PC-I. Two areas corresponding to the layers with the numbers 1 ÷ 14 and 988 ÷ 1000 are presented. It can be seen that the structure of the layers formed in the beginning and in the end of the etching process is different, both the porosity and the thickness of the layers are modified. The period of this structure D_I does not remain constant: periods in the beginning and in the end calculated using fast Fourier transform (FFT) of the SEM images are 160 ± 7 , 150 ± 7 , $131 \pm 7 \text{ nm}$. A continuous decrease of the thickness of each type of PS layers that form the PC with etching depth was observed. In accordance with the calibration measurements described above, this testifies that the r value is decreasing. The spatial period differs much for the first and last etched sets of layers, thus the etching rate also differs much as the thickness of the PS layers is increasing.

On the contrary, in case of PC-II, the SEM images (Fig. 6) of three spatial regions are shown, placed close to the front side, in the middle, and close to the back side of the sample. These images reveal similar microstructure, i.e.,

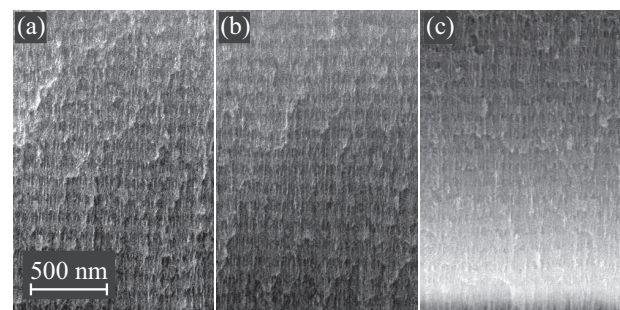


FIG. 6. SEM images of the cross section of porous silicon photonic crystal (PC-II) of 5000 layers (layers are horizontal, etching direction is from top to bottom) (a): for the layers with the numbers 1 ÷ 25 (front side), (b): layers in the middle of the sample, and (c): layers placed close to the back side of the PC.

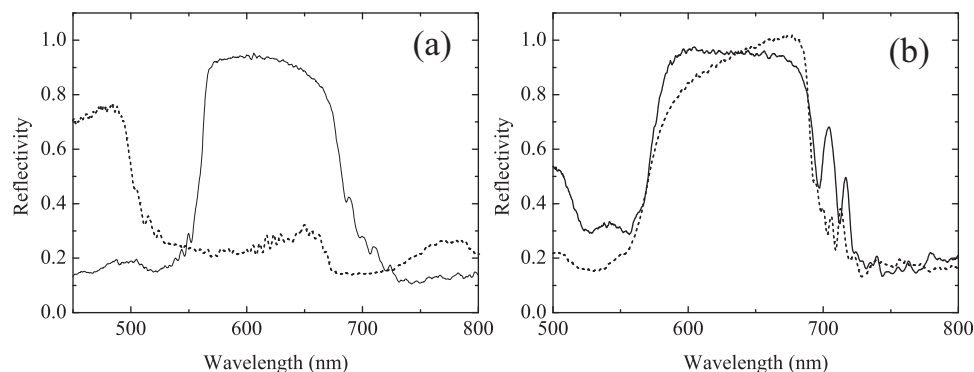


FIG. 7. Reflectivity spectra measured from the front (solid line) and back (dashed line) sides of free-standing photonic crystals fabricated (a) without and (b) when mixing the electrolyte during etching.

the spatial periodicity as well as the diameter of pores are the same. This is also illustrated by the FFT of these images which prove that the spatial period is constant (calculated periods of images are 160 ± 7 nm, 157 ± 7 nm, 150 ± 7 nm, respectively) throughout the structure if the mechanical mixing of the electrolyte is introduced during the etching. Approximate diameters of pores measured in SEM image are $a_1 = 30$ nm and $a_2 = 60$ nm for layers corresponding to current densities of j_1 and j_2 , respectively.

This same conclusion was proven by the direct measurements of the reflectivity spectra measured from the front and back sides of thick free-standing PC fabricated without and in the presence of the solution. Figure 7 shows such spectra measured in case of a PC-2, i.e., made when mixing the electrolyte. One can see that both spectra reveal clear photonic band gaps, which manifest themselves by a spectral region with high reflectivity (low transmittance). What is important here is that the spectral positions of the PBG as well as the reflectivity within the PBG are nearly the same, which proves that such parameters of the PS structure as the spatial periodicity, porosity of the layers, and quality of interfaces remain constant within the structure.

These results prove that the described method of the electrochemical etching can be applied for the composition of PS-based 1D photonic crystals with the number of layers of at least up to 5000. The total time required for this is about 6 h, while there are nearly no technological restrictions for the composition of PC with the desired number of layers and for a given spectral position of the PBG. The main difference between the existing multilayer structures and PS-based ones is that in the latter case there is no mismatch between the crystalline lattices of the neighbouring layers, which is an intrinsic property and a great advantage of porous silicon based structures.

V. ANNEALED POROUS SILICON-BASED PHOTONIC CRYSTALS

One of the main restrictions for the usage of PC is their absorption in the visible spectral range. In case of porous silicon, the transmission of the structure is determined by the volume fraction of silicon which absorbs in the visible spectral range. At the same time, an idea of making a periodical stack of layers on the base of a transparent porous material seems to be very attractive, as there is no principal restriction for the fabrication of large number of layers as there is intrinsically no lattice mismatch between the neighbour

layers. Another dignity of such structures which is also valid in case of nonannealed PS is the possibility to infiltrate their pores by functional materials which may change their refraction index under the external subjections and thus to tune the PBG. These considerations determined the main motivation for the development of the procedure of thermal annealing of porous silicon based structures.

It is known^{18,19} that annealing of crystalline silicon in oxygen atmosphere and at the temperature $T > 900^\circ\text{C}$ leads to the oxidation of Si to SiO_2 . We annealed our PS-based structures under these conditions for 2 h. Reflectivity spectra of the PC prior to and after the thermal annealing are shown in Fig. 9. The sample consisted of 1000 layers with the following parameters: $n_1 = 2.1$, $d_1 = 90$ nm, $n_2 = 1.8$, $d_2 = 100$ nm. The PBG center was attained at $\lambda_0 \approx 740$ nm.

It can be seen that annealed PC also demonstrates the PBG with the reflectivity of about 99%, which proves that the high periodicity of the structure remains. At the same time, a PBG blueshift of about 200 nm is achieved, which is evidently due to the decrease of the PC refractive index as silicon in the porous structure is substituted by amorphous quartz. This transformation can be also noted by eye, as the PC sample after the annealing becomes transparent (glass-like) with a definite changing of colour from yellow to blue under the variation of the angle of incidence.

The estimation of the oxide layer thickness²⁰ for these conditions is about 25 nm.

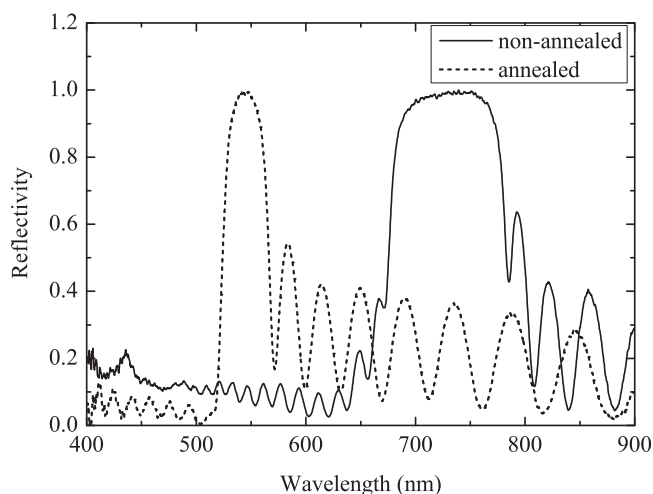


FIG. 8. Reflectivity spectra of the photonic crystal prior to (solid line) and after (dashed line) the thermal annealing.

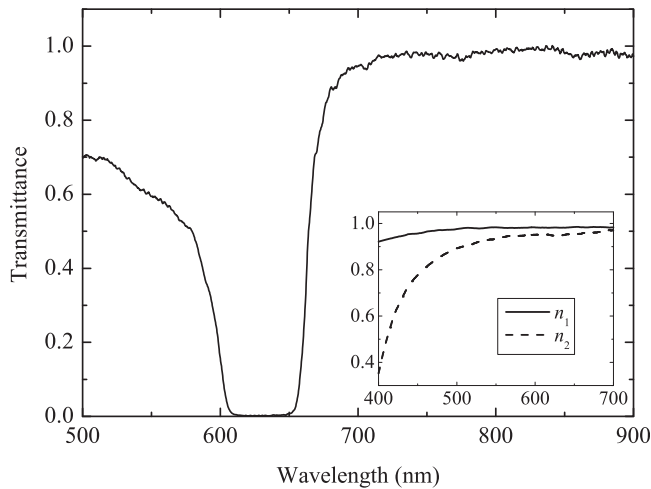


FIG. 9. Transmission spectrum of the annealed porous silicon photonic crystal of 1000 layers (total thickness about $100\ \mu\text{m}$). Inset: transmission spectra of uniform $100\ \mu\text{m}$ layers of annealed porous silicon with the same refractive indices n_1 , n_2 as layers of the photonic crystal.

The estimation of the effective refractive indices of the each PC layer type was made using homogeneous annealed porous silicon films. It shows that the effective values in annealed sample for each type of layer are about $n_1 = 1.48$ and $n_2 = 1.32$, respectively. The thicknesses of films remain unchanged according to accuracy of measurement. This estimation gives the value of the PBG center for the PC with $d_1 = 90\ \text{nm}$, $d_2 = 100\ \text{nm}$ of about $530\ \text{nm}$ which stays in a reasonable agreement with the experimental value (Fig. 8).

Figure 9 shows the transmission spectrum of the annealed PC composed of 1000 layers. This spectrum represents total opaqueness inside band gap region and good uniform transmission beyond it. The decrease of the transmission at short wavelength can be explained as Rayleigh scattering: the transmission of scattering medium is

$$T = \frac{I}{I_0} = e^{-\sigma Nz}, \quad \sigma = \frac{2\pi^5 a^6}{3 \lambda^4} \left(\frac{n^2 - 1}{n^2 + 2} \right)^2, \quad (5)$$

where z is sample thickness, N is concentration of pores, a is pore diameter, λ is wavelength, and n is refraction index. Transmission spectra of uniform $100\ \mu\text{m}$ layers of refraction indices n_1 and n_2 (Fig. 9, inset) can be fitted with the function $f(\lambda) = e^{-A\lambda^{-4}}$ with parameters $A_1 = 2.6 \times 10^{-3}\ \mu\text{m}^4$ and $A_2 = 2.5 \times 10^{-2}\ \mu\text{m}^4$, respectively.

For $z_1 = z_2 = 100\ \mu\text{m}$, $n_1 = 1.48$ and $n_2 = 1.32$, $a_1 = 30\ \text{nm}$ and $a_2 = 60\ \text{nm}$, N_1 , N_2 obtained from porosity calculated by Bruggeman formula 1 and $\lambda = 400\ \text{nm}$, the cross-sections of Rayleigh scattering are $\sigma_1 = 1.4 \times 10^{-15}\ \text{cm}^2$ and $\sigma_2 = 1.5 \times 10^{-13}\ \text{cm}^2$. Corresponding transmission coefficients for $\lambda = 400\ \text{nm}$ are $T_1 = 0.9$ and $T_2 = 0.4$, which match the experimental result (Fig. 9, inset)

VI. SUMMARY

Summing up, we carried out the experimental studies on the composition of porous-silicon based 1D photonic crystals with large number of periods. An important role of

the concentration at fluoric acid inside the pores in the electrochemical etching rate is demonstrated. Good quality of the composed PC structure was confirmed by a comparative study of the reflectivity spectra of the front and the back sides of a thick free-standing PC.

Another issue to be pointed out here is the demonstrated possibility for the fabrication of nearly transparent photonic crystal based on the annealed porous silicon PC. The authors prove that the temperature annealing of such structures results in the formation of fused quartz PCs with good quality of photonic band gap. This opens exciting perspectives for the applications of transparent porous quartz PC with nearly no restriction for the desired spectral range.

ACKNOWLEDGMENTS

Authors acknowledge the financial support from Russian Foundation of Basic Research.

- ¹A. Yariv and P. Yeh, *Optical Waves in Crystals* (Wiley, New York, 1984).
- ²J. D. Joannopoulos, P. R. Villeneuve, and S. H. Fan, "Photonic crystals: Putting a new twist on light," *Nature (London)* **386**, 143–149 (1997).
- ³I. E. Razdol'skii, T. V. Murzina, O. A. Aktsipetrov, and M. Inoue, "Bormann effect in photonic crystals: Nonlinear optical consequences," *JETP Lett.* **87**, 395–398 (2008).
- ⁴D. G. Gusev, I. V. Soboleva, M. G. Martemyanov, T. V. Dolgova, A. A. Fedyanin, and O. A. Aktsipetrov, "Enhanced second-harmonic generation in coupled microcavities based on all-silicon photonic crystals," *Phys. Rev. B* **68**, 4 (2003).
- ⁵L. Pavesi, "Porous silicon dielectric multilayers and microcavities," *Riv. Nuovo Cimento* **20**, 1–76 (1997).
- ⁶V. Lehmann, *Electrochemistry of Silicon: Instrumentation, Science, Materials and Applications* (Wiley-VCH Verlag GmbH, 2002).
- ⁷H. Foll, M. Christophersen, J. Carstensen, and G. Hasse, "Formation and application of porous silicon," *Mater. Sci. Eng. R.* **39**, 93–141 (2002).
- ⁸V. A. Bushuev, B. I. Mantsyzov, and A. A. Skorynin, "Diffraction-induced laser pulse splitting in a linear photonic crystal," *Phys. Rev. A* **79**, 5 (2009).
- ⁹A. E. Antipov and A. N. Rubtsov, "Optical echo in photonic crystals," *JETP Lett.* **85**, 156–159 (2007).
- ¹⁰M. Campbell, D. N. Sharp, M. T. Harrison, R. G. Denning, and A. J. Turberfield, "Fabrication of photonic crystals for the visible spectrum by holographic lithography," *Nature (London)* **404**, 53–56 (2000).
- ¹¹M. Maldovan and E. L. Thomas, "Diamond-structured photonic crystals," *Nature Mater.* **3**, 593–600 (2004).
- ¹²P. Jiang and M. J. McFarland, "Large-scale fabrication of wafer-size colloidal crystals, macroporous polymers and nanocomposites by spin-coating," *J. Am. Chem. Soc.* **126**, 13778–13786 (2004).
- ¹³D. Y. Wang and H. Mohwald, "Rapid fabrication of binary colloidal crystals by stepwise spin-coating," *Adv. Mater.* **16**, 244 (2004).
- ¹⁴A. V. Tikhonravov, M. K. Trubetskoy, and G. W. DeBell, "Application of the needle optimization technique to the design of optical coatings," *Appl. Opt.* **35**, 5493–5508 (1996).
- ¹⁵V. Agarwal and J. A. del Rio, "Tailoring the photonic band gap of a porous silicon dielectric mirror," *Appl. Phys. Lett.* **82**, 1512–1514 (2003).
- ¹⁶D. A. G. Bruggeman, "Calculation of various physics constants in heterogeneous substances i dielectricity constants and conductivity of mixed bodies from isotropic substances," *Ann. Phys.* **24**, 636–664 (1935).
- ¹⁷G. E. Jellison, F. A. Modine, C. W. White, R. F. Wood, and R. T. Young, "Optical properties of heavily doped silicon between 1.5 and 4.1 eV," *Phys. Rev. Lett.* **46**, 1414–1417 (1981).
- ¹⁸L. A. Golovan, V. Y. Timoshenko, and P. K. Kashkarov, "Optical properties of porous-system-based nanocomposites," *Phys. Usp.* **50**, 595–612 (2007).
- ¹⁹J. E. Lugo, H. A. Lopez, S. Chan, and P. M. Fauchet, "Porous silicon multilayer structures: A photonic band gap analysis," *J. Appl. Phys.* **91**, 4966–4972 (2002).
- ²⁰B. E. Deal and A. S. Grove, "General relationship for the thermal oxidation of silicon," *J. Appl. Phys.* **36**, 3770–3778 (1965).